Logical modeling of the mammalian cell cycle

Pauline Traynard[1,2], Adrien Fauré[3], François Fages[2] and Denis Thieffry[1,2]

[1]Computational Systems Biology team, Institut de Biologie de l'Ecole Normale Supérieure (IBENS), CNRS, Inserm, Ecole Normale Supérieure, PSL Research University, Paris, France.

[2]EPI Lifeware, Inria Paris-Rocquencourt, Domaine de Voluceau 78150 Rocquencourt, France.

[3]Graduate School of Science and Engineering, Yamaguchi University, Yamaguchi, Japan.

Abstract

Proper understanding of the behavior of complex biological regulatory networks requires the integration of heterogeneous data into predictive mathematical models. Logical modeling focuses on qualitative data and offers a flexible framework to delineate the main dynamical properties of such networks. However, formal analysis faces a combinatorial explosion as the number of regulatory components and interactions increases.

Here, we show how model-checking techniques can be used to verify sophisticated dynamical properties resulting from model regulatory structure. We demonstrate the power of this approach through the updating of a model of the molecular network controlling mammalian cell cycle. We use model-checking to progressively refine this model in order to fit recent experimental observations. The resulting model accounts for the sequential activation of cyclins, the role of Skp2, and emphasizes a multifunctional role for the cell cycle inhibitor Rb.

1. Introduction

1.1. The logical modeling framework

A logical model is defined by a regulatory graph, where each node represents a regulatory component, and is associated with discrete levels of activity (0, 1, and further integers when justified). Each arc represents a regulatory interaction between the source and target nodes, and is labelled by a threshold and a sign (positive or negative). The dynamical behavior of each node is then defined by logical functions or rules, which associate a target value with this node for each combination of regulators. The dynamics of the system can be represented in terms of a state transition graph (STG), where the nodes denote the states of the system (i.e. vectors giving the levels of activity of all the variables), and the arcs represent state transitions (i.e. changes in the value of one or several variables, according to the corresponding logical functions) (for more details, see Thomas and D'Ari, 1990; Thomas et al., 1995; Chaouiya et al., 2003).

When concurrent variable changes are enabled at a given state, the resulting state transition depends on the chosen updating assumption. With a fully synchronous strategy, all variables are updated through a unique transition. This assumption leads to relatively simple transition graphs and deterministic dynamics. However, this approximation notably leads to spurious cyclic attractors. On the other hand, the fully asynchronous updating assumption considers separately all possible transitions. The resulting dynamics is more difficult to evaluate.

For several years, our group has been developing a software suite, GINsim, to facilitate the definition, the simulation, and the dynamical analysis of logical models (Naldi et al., 2009; Chaouiya et al., 2012). In particular, this software supports STG construction for different updating assumptions. In addition, it provides a function to compress state transition graphs by regrouping the states into components leading to the same attractors or cyclic components, thereby easing the identification of dynamical attractors (stable states, simple or complex cycles) along with their basins of attractions (Bérenguier et al., 2013). Finally, GINsim enables the definition and storage of different initial states and perturbations (e.g. gain- or loss-of-function mutants) (for more details, see the GINsim web site at http://ginsim.org).

In this paper, we focus on the asynchronous updating strategy, which allows the consideration of alternative dynamics in the absence of kinetic data, and we rely on model-checking techniques to analyze the resulting complex transition graph.

1.2. Model-checking

Model checking allows the formal verification of specific dynamical properties and thereby the validation or refutation of a model (Clark et al., 1999). It can also be used to formulate predictions or hypotheses on the studied system. The formalization of dynamical properties can be done using a temporal logic language such as Computation Tree Logics (CTL). Several powerful model-checking tools are available to evaluate CTL specifications on discrete models.

NuSMV is a symbolic model-checker based on Binary Decision Diagrams that provides a description language to specify generic finite state machines, supporting modules and processes (Cimatti et al., 2002). It has been widely used to check properties on discrete regulatory networks. Chabrier & Fages (2003) introduced symbolic model-checking for systems biology using CTL formulae to assess state reachability. Later, Batt et al. (2005) tested conditions leading to a given state, imposing restrictions on sequences of events along the path. In (Batt et al., 2010), model-checking with NuSMV was used to solve a parameter search problem for piecewise-affine differential equation models of regulatory networks in order to reproduce observed expression profiles.

Approaches using extensions of standard CTL have been explored, such as Action Restricted CTL (ARCTL), used to discriminate between variants of a logical model of T-helper cell differentiation, or to investigate reachability properties between stable states subsequent to changes of input conditions (Monteiro et al., 2010; Abou-Jaoudé et al., 2015). Another approach implemented in ANTELOPE (Analysis of Networks through TEmporal-LOgic sPEcifications) (Arellano et al., 2011) supports Hybrid CTL, an extension of standard CTL with a special binder temporal operator, capable of selecting partially characterised states.

Most uses of model-checking for logical modeling so far correspond to reachability properties verifying the existence of a path between a set of initial states and a set of reachable states, with possible restrictions on the paths. Here, we use the model-checker NuSMV to verify the existence or the absence of specific state transition paths corresponding to sophisticated dynamical properties. We use the following generic formula to verify the existence of a sequence States1 → States2 → States3, following any path starting from a state in States1:

INIT States1; SPEC !E[(States1) U (States2 & E[(States2) U (States3)])];

where *States1*, *States2* and *States3* denote sets of states defined by constraints on some of the components of the model, *!* stands for the logical negation, *E* for the existence of a path, and *U* for the until operator.

The negation is used here for two reasons. First, since a CTL temporal logic property φ holds if all initial states satisfy φ, testing whether ¬φ holds verifies the absence of the specified sequence. Second, a contradiction of ¬φ returns an example of transition path matching the prescribed sequence.

In our study, some of the sequences considered are expected to exist in the asynchronous transition graph. Alternatively, we also use sequences representing reactions occurring in an incorrect order and the corresponding dynamical property is then satisfied if the sequence does not exist in the asynchronous STG (cf. Results).

We do not expect all the observed dynamical properties on the cell cycle to be satisfied by our model. Like any model, it is incomplete and relies on approximations and assumptions about the underlying biochemical network. Moreover, in the logical framework, the asynchronous assumption relies on a branching definition of time, potentially resulting in different dynamics compatible with the same model. However, this limitation can be seen as an asset: indeed, a property satisfied in the asynchronous transition graph is intrinsically rooted in the structure of the model, and as such could always be exhibited in some conditions. Properties that are not satisfied do not necessarily indicate a default of the model, but might rather point to specific kinetic constraints.

The cell cycle represents a particularly interesting case, because the maintenance and preservation of distinct phases is a highly complex and coordinated process. It is regulated by protein synthesis,

phosphorylation (through the activity of cyclin-dependent kinases or CDKs) and protein degradation processes (involving ubiquitin ligases). We expect that characteristic dynamical properties, such as checkpoints and irreversible transitions, are robustly encoded in the structure of the corresponding regulatory network. Analysis of a logical model should reveal such properties, despite the absence of detailed kinetic information.

1.3. Logical modeling of the mammalian cell cycle

The cell cycle involves a succession of phases governing genome replication (S phase) and cell division (mitosis or M phase), separated by regulated irreversible transitions (checkpoints). Widely conserved among eucaryotes, the underlying core network has been modeled using differential equations for several species (Yeast, Xenopus, mammals), leading to novel insights into its organization and dynamical properties (see e.g. Novák & Tyson, 2004; Gérard et al. 2009; Ferrel et al., 2011; Tyson & Novák, 2015; and references therein). However, extension and analysis of such differential models become really difficult as the number of experimentally identified components and interactions increases. This lead to the consideration of simpler, qualitative but nevertheless rigorous formal approaches, using discrete formalisms (see e.g. Li et al., 2004; Davidich & Bornhholdt, 2008; Irons, 2009; Fauré et al., 2009; Mombach et al., 2014).

The present study is based on the first Boolean model of the mammalian cell cycle (Fauré et al. 2006), which demonstrated that the logical framework enables the reproduction of important properties of the cell cycle. In order to update and extend this model, we further rely on a recent differential model emphasizing the role of Skp2 (Gérard et al. 2009).

Fauré et al. (2006) defined a Boolean model for the core network driving the entry of mammalian cells into cell cycle, based on the differential model proposed by Novák and Tyson in 2004. For proper logical rules, this model accounts for the existence of a quiescent stable state, as well as for a cyclic attractor characterized by the periodic activities of the four main cyclins, which drive the cell cycle through key transitions by enabling the phosphorylation of a number of substrates by their catalytic partners, the cyclin-dependent kinases (cdks). Cyclin D (called CycD and corresponding to an input in the model) is the main target of the growth factors that push a cell out of its quiescent state to enter the cell cycle. Cyclin E (CycE) regulates the transition between the G1 and S phases. Cyclin A (CycA) controls S phase and its progression into G2 phase. Finally, cyclin B (CycB) is in charge of the transition from G2 phase to the mitosis, and thus triggers the division of the cell before its return to the quiescent state or to G1 phase.

Fauré's model further includes the three main inhibitors of the cell cycle: the retinoblastoma protein Rb, the Cdk inhibitor p27/Kip1 (p27 in the sequel) and the proteasome complex represented by its two co-activators Cdh1 and Cdc20. However, this seminal model considered CycD sufficient to completely inhibit p27 and Rb. Hence, these inhibitors were kept inactive along the whole cyclic attractor, whereas, according to experimental data, these factors should be active in G1 phase, and inactive in the rest of the cell cycle (Rivard et al., 1996; Nelson et al. 1997).

Finally, Fauré's model accounts for the role of the E2 ubiquitin conjugating enzyme UbcH10, which participates in Cdh1 dependent degradation of cyclin A. This extension of the original differential model explains how the auto-ubiquitination of UbcH10 likely prevents cyclin A from degradation by the APC in G1 phase.

Reproducing the results of experimental perturbations is a method of choice to validate a dynamical model. Comparing the asymptotical behavior of a model with or without a perturbation provides interesting insights into the structural properties of the system. Fauré et al. (2006) considered a list of documented perturbations to validate their model. However, the simulations of several perturbations did not match experimental observations. In particular, the effect of a loss-of-function of cyclin E does not seem to be adequately predicted.

2. Results

We have investigated the asynchronous dynamics of Fauré's model using model-checking and perturbation analysis, and we systematically assessed the results to refine and extend this model so that it better matches reported data. In this respect, we first carefully reviewed the literature to identify relevant novel information.
The potential roles of different phosphorylation states of the protein Rb (Lundberg & Weinber, 1998) was considered through the use of a ternary node (i.e. taking the value 0, 1 and 2). We assessed an extension of the model considering the role of Skp2, which links three key inhibitors of the cell cycle and constitutes an additional pathway by which Rb can arrest the progression of the cell cycle (Binné et al., 2007; Liu et al., 2008). The regulatory graph of the updated model is depicted on Figure 1, while the corresponding logical rules are listed in Table 1.

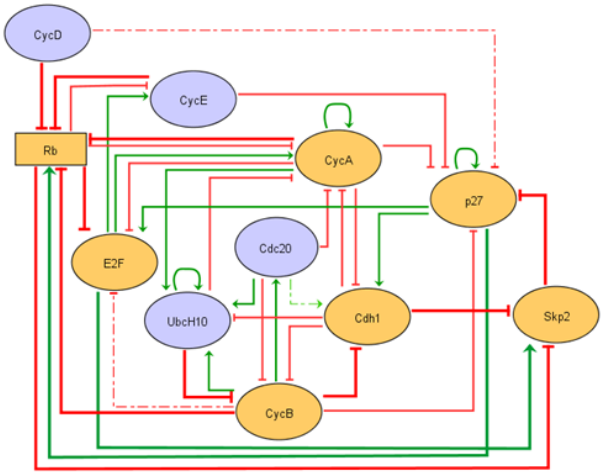

Figure 1. Updated mammalian cell cycle model.
All nodes but Rb are Boolean. Green and red arcs denote positive and negative interactions, respectively. Dashed arrows denote regulations removed from the initial model, while ticker arrows denote added or modified regulations. Orange nodes had their logical functions modified.

Table 1. Logical rules associated with each node of the mammalian cell cycle model (Figure 1). The logical operators NOT, AND and OR are denoted by !, & and |, respectively.

Node	Target value	Logical function
Rb	1	(CycD & !CycE & !CycA & !CycB) | (!CycD & p27 & CycE & CycA & CycB) | (CycD & (CycE | CycA | CycB) & p27)
	2	(!CycD & !CycE & ((!CycA & !CycB) | p27)) | (!CycD & p27 & CycE & (!CycA | !CycB))
E2F	1	(!CycA | p27) & !Rb
CycE	1	E2F & !Rb
CycA	1	(E2F & !Rb | CycA) & !Cdc20 & (!UbcH10 | !Cdh1)
CycB	1	(!UbcH10 | !Cdc20) & !Cdh1
p27	1	(!CycB & (!CycA | p27) & !CycE) | !Skp2
Cdc20	1	CycB
Cdh1	1	(!CycA | p27) & !CycB
UbcH10	1	!Cdh1 | (Cdh1 & UbcH10 & (CycA | Cdc20 | CycB))
Skp2	1	!Cdh1 | (!Rb & E2F)

2.1 Updating of regulatory rules

The cdk inhibitor p27 plays a critical role in several phases of the cell cycle and in the regulation of the quiescent state. It inhibits the activities of cyclin E/cdk2 and cyclin A/cdk2. This inhibitory activity is modeled by opposite regulations on the targets of CycE and CycA. Moreover, p27 and cyclin D also bind in a complex, but this complex retains the activity of cyclin D. Since the cyclins are in competition for complexation with p27, the initial model considered a direct inhibition of p27 by cyclin D to reflect the sequestration of the inhibitor by the cyclin D during the cell cycle. This causes p27 to be completely inactive in presence of the input cyclin D, while it is released and active in absence of the input (i.e. in the quiescent state). This approximation overlooks the role of p27 in the transition from G1 to S. Indeed, the complete activation of cyclin E is a progressive process, slowed down by both Rb and p27, which are both negative regulators of cyclin E: Rb binds to the transcription factor E2F, thereby inhibiting its ability to activate the synthesis of cyclin E, whereas p27 directly binds to cyclin E/Cdk2 and thereby blocks its

activity. Rb and p27 are both phosphorylated by cyclin E, inducing inactivity of Rb and proteasome-dependent degradation of p27. These factors are thus involved in a positive circuit enabling the full activation of the kinase and ultimately entry into S phase (Kotoshiba et al., 2005).

In order to account for this mechanism, we removed the inhibition of p27 by CycD. Although it is clear that cyclin D plays a role in p27 phosphorylation, the observation that the activity of p27 varies in the cell cycle while the level of cyclin D stays consistently high suggests that this role is weak relatively to those of cyclin A, cyclin E and cyclin B (Rivard et al., 1996). Alternatively, a ternary node could be associated with p27 to distinguish two activation levels, in presence versus absence of cyclin D. We have further modified the rule for p27 (see Table 1) to account for the inhibitory effect of CycE (Montagnoli et al., 1999). Simulation of the model with this new rule results in a correct asynchronous attractor with varying p27 activity (in the presence of CycD).

In order to verify the correct role of p27 in the cycle, we check for the existence of the three state transition sequences defined in Table 2. The first represents the expected sequence for the G1/S transition, while the other two correspond to incorrect situations where p27 is either degraded before the activation of its inhibitor CycE, or stays active after the activation of CycA. We further impose the constraint CycB=0 & Cdh1=1 (characteristic of G0) at the initial states.

The requirement of cyclin E for cell cycle viability might depend on the cell context. Cyclin E is known to participate in the phosphorylation of Rb together with cyclin D (Weinberg, 1995). However, observations on cyclin E-deficient cells highlight a crucial role of cyclin E in some situations. Geng et al. (2003) reported that cyclin E-deficient cells can maintain active proliferation but are unable to reenter the cell cycle from the quiescent G0 state. Ohtsubo et al. (1995) further report that inhibition of cyclin E function in G1 blocks the entry in S phase in human cells and arrests the cell cycle.

For CycE knock-out, the simulation of the original model did not result into cell cycle arrest. In contrast, the simulation of our modified model results in an arrest of the cell cycle in phase S, where CycA is inactivated by p27. This simulation emphasizes the role of the Rb-CycE-p27 circuit in driving the cell cycle through the S phase.

A similar perturbation was introduced in a recent study where cancer cells are treated with a specific cyclinE/cyclinA-cdk2 inhibitor, resulting in a cell cycle arrest with an increased accumulation of p27 and hypophosphorylation of Rb (Dai et al., 2013). The simulation of a double perturbation of CycE and CycA for the revised model is consistent with the reported results, while the same perturbation in the initial model results in a cell cycle arrest but with phosphorylated Rb (Rb=0) and no p27 accumulation (p27=0).

Careful reconsideration of each regulation rule further led us to remove the inhibition of E2F by CycB. Although E2F has been shown to be inhibited by cyclin A through direct binding, this is not the case for cyclin B (Krek et al., 1994). Interestingly, the delay between the degradation of cyclin B after the mitosis and the activation of cyclin E during G1-phase was ensured by this regulation. In the updated model, this dynamical property is no longer satisfied, and the example sequence provided by the model-checker confirms that it is due to the activation of E2F before the degradation of cyclin B (cf. sequence 16 in appendix). This is a case of model over-fitting, where an expected dynamical property has been enforced with a hypothetical mechanism unsupported by experiments.

Table 2. Model-checking assessment of alternative dynamics for the G1/S transition

Phenotype	The phosphorylation and subsequent degradation of p27 by cyclin E is necessary to drive the feedforward loop that ensures that cells advance to S-phase irreversibly.								
Sequence	CycE	CycA	p27	CycE	CycA	p27	CycE	CycA	p27
	0	0	1	0	0	1	0	0	1
	1	0	1	0	0	0	1	0	1
	1	0	0	1	0	0	1	1	1
	1	1	0	1	1	0	1	1	0
	0	1	0	0	1	0	0	1	0
Expected result	True			False			False		
Updated model	True ✔			False ✔			False ✔		

We further modified the regulatory rule defining an activation of Cdh1 by Cdc20. These two substrate adaptor proteins of the anaphase-promoting complex (APC) are activated in turn during the G2 and M phases to activate the degradation of mitotic cyclins A and B. Since Cdc20 participates in degrading CycA, which inhibits Cdh1 by phosphorylation, there is an indirect activation of Cdc20 by Cdh1. As Cdh1 has a broader spectrum than Cdc20, it completes CycA and CycB inactivation, and inactivates Cdc20 (Meyer & Rape, 2011). We have thus verified that the direct activation of Cdh1 by Cdc20 could be eliminated without impacting on relevant model properties (cf. Tables 1 to 7 and appendix).

2.2. Multiple forms and roles of Rb

The protein Rb is a major cell cycle inhibitor and tumor suppressor. It is regulated by numerous stimuli that are channeled through Cdk regulation of Rb phosphorylation. The unphosphorylated protein binds to the transcription factor E2F, thereby acting as a growth suppressor and preventing progression through the cell cycle. When phosphorylated, Rb releases E2F, which activates the synthesis of CycE and CycA. Recent findings show that the phosphorylation of Rb is a progressive process (Henley et al., 2012). The phosphorylation of Rb begins in early G1-phase with cyclin D/cdk4 or 6 (Narasimha et al., 2014). This allows some E2Fs to be released and initiates the transcription and subsequent production of cyclin E. The cyclin E/cdk2 kinase activity is able to hyper-phosphorylate Rb. As the majority of phosphorylation sites on Rb need to be modified to abrogate E2F binding, it defines differential activities for the different phosphorylation levels of Rb and a necessary role for cyclin E to drive the cell cycle into S-phase. Rb is maintained hyper-phosphorylated by cyclin A/cdk2 and cyclin B/cdk1 in S, G2, and M phases.

Refining the description of Rb with a multivalued node was already suggested in (Fauré et al., 2006). We thus introduced a ternary node for Rb. The levels 0, 1 and 2 represent the hyper-phosphorylated, partially-phosphorylated and unphosphorylated states respectively. The logical rules for each level are defined in Table 1. The cyclins phosphorylate and inhibit Rb. In absence of cyclins, Rb is unphosphorylated (level 2). CycD alone initiates the partial phosphorylation at the beginning of the cell cycle, and thus leads Rb down to the level 1. It requires the assistance of another cyclin to complete the phosphorylation, leading Rb down to the level 0 in absence of p27. CycA and CycB have symmetrical roles and both of them keep Rb hyperphosphorylated during S, G2 and M phases. p27 binds to the cyclin-cdk complexes and inhibits the kinase activities, playing the role of an indirect activator of Rb. However, although it binds to CycD/Cdk4, the activity of this complex is not impaired. We take into account the saturation of p27 by the different cyclins trough additive and saturation effects.

Interestingly, this model extension provides a mechanism explaining the sequential synthesis of cyclin E and cyclin A. The synthesis of both cyclins is activated by E2F, but their expressions peak in G1 phase and in S phase respectively (Lees et al., 1992; Wong et al., 2014). We propose to model this difference of activation by different effects of the phosphorylated states of Rb. The complexation of Rb and E2F is modeled with a direct inhibition of E2F by Rb but also a negative regulation of Rb on the E2F targets CycE and CycA (as in Fauré et al., 2006). Setting different thresholds of activity for these interactions, namely threshold 2 for E2F and CycE, and threshold 1 for CycA, ensures that the synthesis of CycA can only be activated once Rb is hyperphosphorylated and E2F is completely released.

Table 3. Alternative dynamics for G1/S transition

Phenotype	Cyclin A expression is delayed relative to E2F and cyclin E.	
Sequence	CycE, CycA, CycE, CycA	
	0, 0, 0, 0	
	1, 0, 0, 1	
	1, 1, 1, 1	
Expected result	True	False
Initial model	True ✔	True ✗
Updated model	True ✔	False ✔

Table 4. Role of UbcH10 in mitosis

Phenotype	UbcH10 is required for mitotic cyclin destruction.
Sequence	CycA, CycB, Cdc20, UbcH10
	1, 0, 0, 0
	1, 1, 0, 0
	1, 1, 1, 0
	0, 1, 1, 0
	0, 0, 1, 0
	0, 0, 0, 0
Expected result	False
Initial model	True ✗
Updated model	False ✔

The delayed synthesis of CycA relatively to the synthesis of CycE can be verified by model-checking. A sequence with the reverse order is checked in Table 3, and the result is compared with the initial model. Initially both sequences of the table existed in the asynchronous STG, showing the lack of preferential order of activation between CycE and CycA. After the modification of the model described above, the incorrect sequence with CycA activated before CycE no longer exists in the asynchronous STG. Hence, our model provides an explanation for the observed sequential activation of cyclin E and cyclin A in the cell cycle, which relies on a robust mechanism encoded in the logical structure of the model. This mechanism is based on the feedforward motif that drives the complete phosphorylation of Rb and the progression into S phase.

2.3. Role of UbcH10 in mitosis

The anaphase-promoting complex (APC) coordinates mitosis and G1 by sequentially promoting the degradation of key cell-cycle regulators. APC is represented in the model by the two co-activators Cdh1 and Cdc20. The degradation of several targets of either Cdh1 or Cdc20 is assisted by the ubiquitin-conjugating enzyme 2C (UbcH10, also called UBE2C), a component of the ubiquitin proteasome system.

While the initial model encoded the fact that UbcH10 is necessary for Cdh1-dependent degradation of Cyclin A (Rape & Kirshner, 2004), UbcH10 might also be required for the destruction of mitotic cyclins and other mitosis-related substrates, including cyclin B (Rape et al., 2006). We encoded this putative mechanism by updating the logical rule associated with the node CycB (cf. Table 1). Adding the intervention of UbcH10 for the degradation of CycB enables a consistent simulation of UbcH10 KO.

Indeed, using model-checking, one can verify that there is no asynchronous sequence going through G2 and M phase (driven by cyclin A and cyclin B) in absence of UbcH10 (starting from initial states with Cdh1=1 and Rb=0, corresponding to S phase) (Table 4).

UbcH10 is probably involved also in Cdh1-dependent degradation of CycB. In the absence of definitive experimental data, we can test the impact of this mechanism on cell cycle dynamics using model checking on model variants with alternative rules for CycB. As shown in Table 5, for the second rule considered, CycB can be activated at the beginning of the cell cycle in presence of Cdh1 because UbcH10 has been degraded at the end of the previous cycle.

Table 5. Irreversibility of mitosis

Phenotype	CycB should not be able to increase during G1-phase		
Sequence		CycE	CycB
		0	0
		0	1
Expected result		False	
Rule for CycB: (!UbcH10 | !Cdc20) & !Cdh1		False ✔	
Rule for CycB: !UbcH10 | (!Cdc20 & !Cdh1)		True ✗	

2.4. Role of Skp2

Within the logical framework, it is relatively easy to extend a model to consider novel regulatory components and interactions. Here, we set to include an additional cell cycle inhibitory pathway. Indeed, recent evidence point to the existence of an E2F-independent proliferative control mechanism, which involves the F-box protein Skp2, a substrate recognition subunit of the SCP ubiquitin ligase complex that targets p27 for degradation (Dick & Rubin, 2013). Briefly, Skp2 promotes the degradation of phosphorylated p27, thus enabling its degradation induced by CycE and CycA. Rb binds to Cdh1 to participate in the ubiquitin-mediated degradation of Skp2 (Binné et al., 2007; Liu et al., 2008). This mechanism links the two cell cycle repressors Rb and p27, and provides an additional mechanism by which Rb can arrest the cell cycle.

Consequently, we added a novel node representing Skp2 in the model, negatively regulated by Cdh1 and by non-phosphorylated Rb. The observation that E2F directly activates transcription of skp2 gene (Assoian & Yung, 2008) led us to include a positive regulation by E2F opposing the inhibition by Rb. The performances of this revised model have been validated by checking consistency between simulated perturbations and experimental data. Ji and collaborators (2004) described the partial penetrance Rb mutation RbR661W, which impedes E2F repression, and effectively shuts down the Rb-E2F pathway. The authors further found that RbR661W retains the ability to arrest the cell cycle at the G1/S transition, with a p27 accumulation. They verified that Rb's ability to interact with Skp2-p27 was preserved in this mutant. Using the software GINsim, it is possible to model this subtle perturbation by specifically suppressing the regulation of E2F, CycE and CycA by Rb.

The authors further performed kinetic studies and showed that the Rb-induced G1 cell cycle arrest is initiated by the up-regulation of p27, which inhibits the kinase activity associated with cyclins E and A before the decline of protein levels. The cell cycle is still arrested through the (slower) repression of E2F target genes. Using the aforementioned perturbation, we could assess the early effect of the induction of Rb (Table 6), leading to simulation results consistent with published experimental results (Ji & Zhu, 2005).

In another experiment, the p27 antisense treatment prevents G1 arrest by Rb, showing that p27 is required for Rb-mediated G1 arrest. This can be modeled by considering another constraint (knock-down of p27) in the perturbation simulation, leading to a result consistent with experimental data.

Table 6. Selected perturbations characterizing the Rb-Skp2-p27 pathway

Experiment	Phenotype	Initial model	Updated model
RbR661W	Viable cell cycle in presence of growth factors, cell cycle arrest in absence with p27 accumulation	✗	✔
Rb induction (early kinetics)	Cell cycle arrest with present CycE and CycA	✗	✔
p27 KO (early kinetics)	Cell cycle in absence of growth factors	✗	✔
Skp2 KO	Cell cycle arrest or endoreplication with accumulation of cyclin E and p27.	-	✔
Skp2 KO p27 KO	Cell cycle in presence of growth factors, cell cycle arrest in absence	-	✔

Moreover, Skp2 specific perturbations have been reported in the literature, which can also be qualitatively reproduced with our model. In particular Skp2 KO has been shown to lead to severe proliferation defects with accumulation of both cyclin E and p27 (Kotoshiba et al., 2014; Nakayama et al., 2000). Consistently, the simulation of this perturbation leads to a steady state with CycE and p27 both active (level 1).
Furthermore, the accumulation of cyclin E in this mutant has been interpreted by the suppression of cyclin E degradation. However, the negative regulation of cyclin E by Skp2 is not represented in our model because CycE represents the complex cyclin E/Cdk2. Skp2 is known to degrade free cyclin E, while cyclin E complexed with Cdk2 is protected from Skp2-dependent degradation. This suggests an alternative mechanism by which CycE is accumulated in Skp2 mutants, presumably involving p27 binding to CycE. This complexation could inhibit CycE activity and arrest the cell cycle before the transition toward S phase. The rescue of Skp2 loss-of-function by the deletion of p27 (Kotoshiba et al., 2014) is also correctly reproduced by the model.
Finally, using model-checking, we could verify that the asynchronous dynamics of the updated model is compatible with the observed sequence of periodic variations of all the proteins encompassed by the model (Table 7).

Table 7: Correct asynchronous sequence for a complete cell cycle. The rows denote successive states along the cell cycle, with the active nodes in gray and inactive nodes in white.

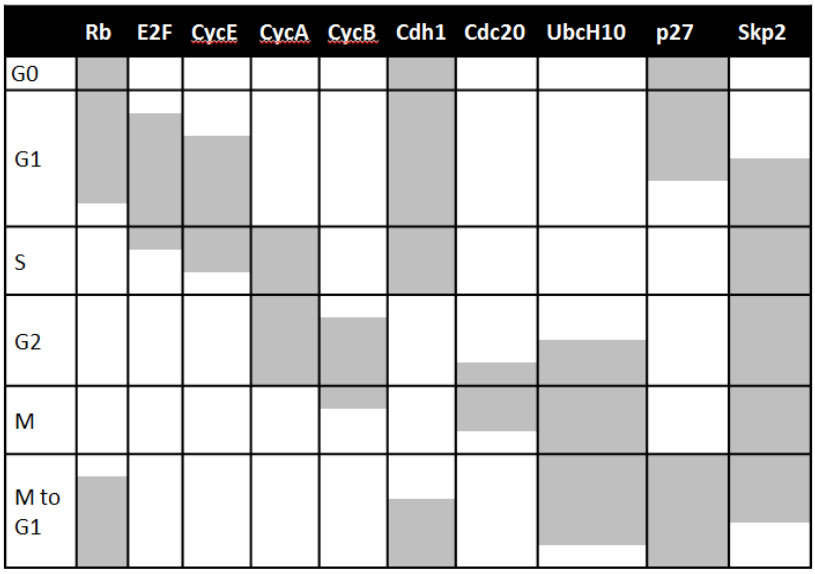

3. Conclusions and prospects

3.1. Model refinement

We have refined a logical model of the mammalian cell cycle to include recent data pointing to novel regulatory components and interactions. Each model update was evaluated using model-checking to assess the conservation of documented dynamical properties, for the wild type cycle and for various genetic perturbations. Refining a model is an iterative process, and while we have focused here on the satisfaction of novel dynamical properties, it is as important to check at each step that all relevant properties satisfied by the original model are not altered. In appendix, we provide a complete list of the perturbations (Table S1) and dynamical properties (Table S2) evaluated on the initial and final models, along with their assessment for both models. As can be seen in these tables, the updated model complies with several additional properties, thereby constituting a clear improvement over the original one.

A careful model checking analysis of our current model already points to some limitations. In particular, the order of activation or degradation of CycB relatively to the other cyclins is not properly determined (see appendix). This raises the question of what refinement could ensure the correct sequential order between cyclin B and the other cyclins. Relevant perturbation studies could bring an insight into possible mechanisms. For examples, the use of stabilized cyclins in proliferating cells could help to conclude whether the degradation of cyclin E, cyclin A and cyclin B are necessary for the progression into the next phase. Alternatively, more subtle kinetic aspects might be responsible for the temporal regulation of cyclin B, which would then require the use of more quantitative approaches.

3.2. Prospects

Our current model takes into account the most notable components of the mammalian cell cycle network. However, this model should be further updated in the light of novel experimental data. For example, several proteins have been involved in the regulation of the G2 phase, such as Aurora, Plk1, Emi1, but have not been yet included in our model because their role or regulation are still uncertain. These factors could be incorporated in the model once more precise mechanistic information becomes available.

Our model could also be refined to fit data concerning specific cell types, or to study the effect of multiple perturbations associated with cancer (e.g. Grieco et al., 2013; Mombach et al., 2014). It can be used as a starting point for subsequent studies, using the model checking approach delineated here in order to increment and assess successive model versions. In this respect, we provided our current model in two computer readable formats (an archive that can be opened using GINsim, along with an SBML export) as supplementary material (http://ginsim.org/node/189). These files include extensive annotations and links to external databases, thereby documenting all components and interactions.

Finally, although the consideration of multivalued nodes is useful to represent multifunctional proteins such as Rb, the analysis of logical models with multivalued nodes can be difficult and is partly supported by a limited number of tools. To enable the import of our model in purely Boolean modelling tools, we further provide a Boolean version of our multivalued model, where the node Rb is split into two Boolean nodes Rb1 and Rb2 (http://ginsim.org/node/189). In particular, this Boolean model can be used to perform stochastic simulations using the software MaBoSS (http://maboss.curie.fr), provided that the user define transition rates for component (up or down) update. Such stochastic simulations have the potential to provide more quantitative characterizations of asymptotic behaviors, for wild type versus perturbed conditions.

6. Acknowledgements

This work has received support under the program « Investissements d'Avenir » launched by the French Government and implemented by ANR with the references ANR-10-LABX-54 MEMOLIFE and ANR-11-IDEX-0001-02 PSL* Research University.

PT has been funded by an AMX doctoral grant from the Ministère de l'Education Nationale, de l'Enseignement Supérieure et de la Recherche.

5. References

Abou-Jaoudé et al (2015). *Front Bioeng Biotechnol* **2**: 86.
Arellano et al (2011) *BMC Bioinformatics* **12**: 490.
Assoian & Yung (2008) *Cell Cycle* 7: 24-7.
Batt et al (2005) *Bioinformatics* **21**: i19-28.
Batt et al (2010) *Bioinformatics* **26**: i603-10.
Bérenguier et al (2013) *Chaos* **23**: 025114.
Binné et al (2007) *Nat Cell Biol* **9**: 225-32.
Bornholdt S (2008) *J R Soc* **5**: S85-94.
Chabrier N & Fages F (2003) *Lect Notes Comput Sci* **2602**: 149-62.
Chaouiya C et al (2003) *Lect Notes Control Infor* **294**: 119-26.
Chaouiya C et al (2012) *Meth Mol Biol* **804**: 463-79.
Cimatti A et al (2002) *Lect Notes Comput Sci* **2404**: 359-64.
Clarke E et al (1999) *Model Checking* Cambridge: MIT Press.
Dai et al (2013) *Cancer Letters* **333**: 103-12.
Davidich M & Bornholdt S (2008) *J Theor Biol* **255**: 269-77.
Dick & Rubin (2013) *Mol Cell Biol* **14**: 297-306.
Fauré A et al (2006) *Bioinformatics* **22**: 124-31.
Ferrell et al (2011) *Cell* **144**: 874-85.
Gérard & Goldbeter (2009) *Proc Natl Acad Sci USA* **106**: 21643-8.
Geng et al (2003) *Cell* **114**:431-43
Grieco et al (2013) *PLoS Comput Biol* **9**: 21003286.
Henley et al (2012) *Cell Div* **7**: 10
Irons J (2009) *J Theor Biol* **257**: 543-59.
Ji et al (2004) *Mol Cell* **16**: 47-58.
Ji & Zhu (2005) *Cell Cycle* **4**: 373-5.
Kotoshiba et al (2014) *Biochim Biophys Acta* **1843**: 436-45.
Krek et al (1994) *Cell* **78**: 161-72.
Lees et al (1992) *Genes Dev* **6**: 1874-85.
Li et al (2004) *Proc Natl Acad Sci USA* **101**: 4781-6.
Liu et al (2008) *Cancer Res* **68**: 9015-23.
Lundberg & Weinberg (1998) *Mol Cell Biol* **18**:753-61.
Meyer & Rape (2011) *Sem Cell Dev Biol* **22**: 544-50.
Mombach et al (2014) *BMC Genomics* **15:** S7.
Montagnoli et al (1999) *Genes Dev* **13**: 1181–89.
Nakayama et al (2000) *The EMBO Journal* **19**: 2069-81.
Naldi et al (2009) *Biosystems* **97**: 134-9.
Narasimha et al. (2014). *eLife* **3**:e02872.
Nelson et al. (1997) *J Biol Chem* **272**:4528-4535.
Novák & Tyson (2004) *J Theor Biol* **230**: 563-79.
Ohtsubo et al. (1995) *Mol Cell Biol* **15**: 2612-24.
Rape et al. (2006) *Cell* **124**: 89-103.
Rivard et al (1996) *J Biol Chem* **271**: 18337-41.
Thomas R & D'Ari R (1990) *Biological Feedback*. Boca Raton: CRC Press.
Thomas et al (1995) *Bull Math Biol* **57**: 247-76.
Townsley et al (1997) *Proc Natl Acad Sci USA* **94**: 2362-7.
Tyson & Novák (2015) *BMC Biol* **13**: 46.
Weinberg (1995) *Cell* **81**: 323-30.
Wong et al (2014) *Cell Cycle* **10**: 3086-94.

Appendix

Table S1. P**erturbation simulations**

Experiment	Phenotype	Fauré et al. (2006)	Updated model
p27 KO	cycle in absence of growth factor	**Disagreement**	**Disagreement**
CycE E1	Viable; cycle in absence of growth factor; less serum-dependent.	For CycD=0, cycle or steady state. Questionable	Cycle for CycD=1, steady state for CycD=0. Questionable
p27 E1	Cell cycle arrest in presence of growth factors.	OK	OK
p27 and CycA E1	Cell cycle arrest in presence of growth factors.	OK	OK
p27 and CycE E1	Cell cycle arrest in presence of growth factors.	OK	OK
p27 and E2F E1	Cell cycle arrest in presence of growth factors.	OK	OK
Rb E2	G1 arrest + p27 accumulation	OK	OK
Cdh1 KO	Viable cell cycle in presence or absence of growth factors.	OK	OK
UbcH10 KO	Cell cycle arrested in M phase, destruction of cyclin A and B inhibited.	**Disagreement**	OK
E2F overexpression in Rb-/- E2F E1 Rb KO	Viable cell cycle in presence or absence of growth factors	OK	OK
E2F overexpression in Rb+/+ E2F E1 Rb E1 CycE [Rb@0] CycA [Rb@0]	Targets of E2F are expressed even in absence of growth factor but the cell cycle is arrested.	Cyclic attractor with CycD=0 or CycD=1 **Disagreement**	OK
Loss of Rb Rb KO	Viable cell cycle in presence or absence of growth factors	OK	OK
Rb induction (early kinetics) Rb E1 E2F [Rb@0] CycE [Rb@0] CycA [Rb@0]	Cell cycle arrest	Cyclic attractor with CycD=0 or CycD=1 **Disagreement**	OK
RbR661W E2F [Rb@0] CycE [Rb@0] CycA [Rb@0]	Cell cycle in presence of growth factors, cell cycle arrest in absence	Cyclic attractor with CycD=0 or CycD=1 **Disagreement**	OK
p27 KO (early kinetics) Rb E1 p27 KO E2F [Rb@0] CycE [Rb@0] CycA[Rb@0]	Viable cell cycle in presence or absence of growth factors	OK	OK
Skp2 KO	Cell cycle arrest or endoreplication with Cyclin E and p27 accumulation.	-	OK
Skp2 KO p27 KO	Cell cycle in presence of growth factors, cycle arrest in absence	-	OK
Skp2 overexpression and Rb induction (early kinetics) Skp2 E1 Rb E2 E2F [Rb@0] CycE [Rb@0] CycA [Rb@0]	Viable cell cycle in presence or absence of growth factors.	-	OK

Table S2. Verification of dynamical properties with model-checking

Phenotypes	Sequences of events verified by model-checking	Fauré et al. (2006)	Updated model
Feedforward loop that ensures that cells advance to S-phase irreversibly : phosphorylation of Rb by CycE to release E2F and synthetise more CycE, and phosphorylation of p27.	**1.** Correct sequence: CycE=0 & CycA=0 & p27=1 -> CycE=1 & CycA=0 & p27=1 -> CycE=1 & CycA=0 & p27=0 -> CycE=1 & CycA=1 & p27=0 -> CycE=0 & CycA=1 & p27=0	**No**	OK
	2. Incorrect sequence starting from CycB=0 & Cdh1=1 (G1) or Rb=1 & CycB=0 & Cdh1=1 for the updated model: CycE=0 & CycA=0 & p27=1 -> CycE=0 & CycA=0 & p27=0 -> CycE=1 & CycA=0 & p27=0 -> CycE=1 & CycA=1 & p27=0 -> CycE=0 & CycA=1 & p27=0	**No**	OK
	3. Incorrect sequence starting from CycB=0 & Cdh1=1 (G1) or Rb=1 & CycB=0 & Cdh1=1 for the updated model: CycE=0 & CycA=0 & p27=1 -> CycE=1 & CycA=0 & p27=1 -> CycE=1 & CycA=1 & p27=1 -> CycE=1 & CycA=1 & p27=0 -> CycE=0 & CycA=1 & p27=0	**No**	OK
	4. Incorrect sequence starting from CycB=0 & Cdh1=1 (G1) or Rb=1 & CycB=0 & Cdh1=1 for the updated model: CycE=0 & CycA=0 & p27=1 -> CycE=1 & CycA=0 & p27=1 -> CycE=1 & CycA=0 & p27=1 -> CycE=1 & CycA=1 & p27=1 -> CycE=0 & CycA=1 & p27=1	OK	OK
As long as E2F is inactivated, the cell remains in the G1 phase.	**5.** Incorrect sequence starting from CycB=0 & Cdh1=1 (G1) or Rb=1 & CycB=0 & Cdh1=1 for the updated model: CycE=0 & CycA=0 & p27=1 & E2F=0 -> CycE=1 & CycA=0 & p27=1& E2F=0 -> CycE=1 & CycA=0 & p27=0 & E2F=0 -> CycE=1 & CycA=1 & p27=0 & E2F=0 -> CycE=0 & CycA=1 & p27=0 & E2F=0	OK	OK
Cyclin A expression is delayed relative to E2F and cyclin E.	**6.** Incorrect sequence starting from CycB=0 & Cdh1=1 (G1) or Rb=1 & CycB=0 & Cdh1=1 for the updated model: CycE=0 & CycA=0 & E2F=0 -> CycE=0 & CycA=0 & E2F=1 -> CycE=1 & CycA=0 & E2F=1 -> CycE=1 & CycA=0 & E2F=0 -> CycE=1 & CycA=1 & E2F=0 -> CycE=0 & CycA=1 & E2F=0	OK	OK
Sequential activation of CycE and CycA.	**7.** Incorrect sequence starting from CycB=0 & Cdh1=1 (G1) or Rb=1 & CycB=0 & Cdh1=1 for the updated model: CycE=0 & CycA=0 -> CycE=0 & CycA=1 -> CycE=1 & CycA=1	**No**	OK
Degradation of B cyclins by the APC/C complex is required for mitosis to take place.	**8.** Correct sequence from Rb=0 & Cdh1=0 & p27=0 & Skp2=1 & CycE=0 (G2): CycA=1 & CycB=0 & Cdc20=0 -> CycA=1 & CycB=1 & Cdc20=0 -> CycA=1 & CycB=1 & Cdc20=1 -> CycA=0 & CycB=1 & Cdc20=1 -> CycA=0 & CycB=0 & Cdc20=1 -> CycA=0 & CycB=0 & Cdc20=0	OK	OK
	9. Incorrect sequence from Rb=0 & Cdh1=0 & p27=0 & Skp2=1 & CycE=0 (G2): CycA=1 & CycB=0 & Cdc20=0 -> CycA=1 & CycB=1 & Cdc20=0 -> CycA=1 & CycB=1 & Cdc20=1 -> CycA=0 & CycB=1 & Cdc20=1 -> CycA=0 & CycB=1 & Cdc20=0 -> CycA=0 & CycB=0 & Cdc20=0		
	10. Incorrect sequence from Rb=0 & Cdh1=0 & p27=0 & Skp2=1 & CycE=0 (G2): CycA=1 & CycB=0 & Cdc20=0 -> CycA=1 & CycB=1 & Cdc20=0 ->CycA=0 & CycB=1 & Cdc20=0 ->CycA=0 & CycB=0 & Cdc20=0; CycA=1 & CycB=0 -> CycA=1 & CycB=1 ->CycA=1 & CycB=0 ->CycA=0 & CycB=0		
Cdh1 is not required for mitotic exit.	**11.** Correct sequence from Rb=0 & Cdh1=0 & p27=0 & Skp2=1 & CycE=0 (G2): CycA=1 & CycB=0 & Cdc20=0 & Cdh1=0 -> CycA=1 & CycB=1 & Cdc20=0 & Cdh1=0 -> CycA=1 & CycB=1 & Cdc20=1& Cdh1=0 -> CycA=0 & CycB=1 & Cdc20=1& Cdh1=0 -> CycA=0 & CycB=0 & Cdc20=1 & Cdh1=0 -> CycA=0 & CycB=0 & Cdc20=0 & Cdh1=0	OK	OK

UBEC2 is required for the destruction of mitotic cyclins and other mitosis-related substrates.	**12.** Incorrect sequence from Rb=0 & Cdh1=0 & p27=0 & Skp2=1 & CycE=0 (G2) : CycA=1 & CycB=0 & Cdc20=0 & UbcH10=0 -> CycA=1 & CycB=1 & Cdc20=0 & UbcH10=0 -> CycA=1 & CycB=1 & Cdc20=1& UbcH10=0 -> CycA=0 & CycB=1 & Cdc20=1& UbcH10=0 -> CycA=0 & CycB=0 & Cdc20=1 & UbcH10=0 -> CycA=0 & CycB=0 & Cdc20=0 & UbcH10=0	**No**	OK
Degradation of CycE in S phase, activation of CycB in G2 phase	**13.** Incorrect sequence starting from CycB=0 & Cdh1=1 (G1) or Rb=1 & CycB=0 & Cdh1=1 for the updated model: CycE=0 & CycA=0 & CycB=0 -> CycE=1 & CycA=0 & CycB=0 -> CycE=1 & CycA=1 & CycB=0 -> CycE=1 & CycA=1 & CycB=1 -> CycE=0 & CycA=1 & CycB=1 -> CycE=0 & CycA=0 & CycB=1 -> CycE=0 & CycA=0 & CycB=0	**No**	**No**
Synthesis of CycA in in early S phase, activation of CycB in G2 phase.	**14.** Incorrect sequence starting from CycB=0 & Cdh1=1 (G1) or Rb=1 & CycB=0 & Cdh1=1 for the updated model: CycE=0 & CycA=0 & CycB=0 -> CycE=1 & CycA=0 & CycB=0 -> CycE=1 & CycA=0 & CycB=1 -> CycE=1 & CycA=1 & CycB=1	OK	OK
Degradation of CycA in early mitosis, degradation of CycB in late mitosis	**15.** Incorrect sequence starting from CycB=0 & Cdh1=1 (G1) or Rb=1 & CycB=0 & Cdh1=1 for the updated model: CycE=0 & CycA=0 & CycB=0 -> CycE=1 & CycA=0 & CycB=0 -> CycE=1 & CycA=1 & CycB=0 -> CycE=0 & CycA=1 & CycB=0 -> CycE=0 & CycA=1 & CycB=1 -> CycE=0 & CycA=1 & CycB=0 -> CycE=0 & CycA=0 & CycB=0	**No**	**No**
Complete removal of cyclin B1 is essential to prevent the return of the spindle checkpoint following sister chromatid disjunction.	**16.** Incorrect sequence starting from CycB=0 & Cdh1=1 (G1) or Rb=1 & CycB=0 & Cdh1=1 for the updated model: CycE=0 & CycA=0 & CycB=0 ->CycE=1 & CycA=0 & CycB=0 ->CycE=1 & CycA=1 & CycB=0 ->CycE=0 & CycA=1 & CycB=0 ->CycE=0 & CycA=1 & CycB=1 ->CycE=0 & CycA=0 & CycB=1 ->CycE=1 & CycA=0 & CycB=1	OK	**No**
Experimentally observed expressions of each component	**17.** Correct sequence defined in Table 9	OK for a sequence without p27, Rb and Skp2	OK